Mechanical and structural model of fractal networks of fat crystals at low deformations

Suresh S. Narine and Alejandro G. Marangoni
Department of Food Science, University of Guelph, Guelph, Ontario, Canada N1G 2W1
(Received 25 March 1999; revised manuscript received 14 June 1999)

Fat-crystal networks demonstrate viscoelastic behavior at very small deformations. A structural model of these networks is described and supported by polarized light and atomic-force microscopy. A mechanical model is described which allows the shear elastic modulus (G') of the system to be correlated with forces acting within the network. The fractal arrangement of the network at certain length scales is taken into consideration. It is assumed that the forces acting are due to van der Waals forces. The final expression for G' is related to the volume fraction of solid fat (Φ) via the mass fractal dimension (D) of the network, which agrees with the experimental verification of the scaling behavior of fat-crystal networks [S. S. Narine and A. G. Marangoni, Phys. Rev. E **59**, 1908 (1999)]. G' was also found to be inversely proportional to the diameter of the primary particles ($\sigma \approx 6\ \mu$m) within the network (microstructural elements) as well as to the diameter of the microstructures ($\xi \approx 100\ \mu$m) and inversely proportional to the cube of the intermicrostructural element distance (d_0). This formulation of the elastic modulus agrees well with experimental observations.
[S1063-651X(99)14511-2]

PACS number(s): 61.43.−j, 61.41.+e, 83.20.Bg, 83.50.Fc

I. INTRODUCTION

Plastic fats demonstrate rheological properties such as a yield value and viscoelastic behavior as a result of a crystal network formed within such systems. The fat behaves like a rigid solid until the deforming stress exceeds the yield value and the fat starts flowing like a viscous liquid [1]. Furthermore, many of the important quality characteristics of fat-containing food products depend on the macroscopic rheological properties of the fat-crystal network formed within the finished product. Some of these characteristics include the spreadability of margarine, butter and spreads, as well as the snap of chocolate. Predicting the macroscopic rheological properties of fat-crystal networks within these products is therefore important not only from a fundamental perspective, but from an industrial perspective as well.

Structural models to predict the rheological nature of fat-crystal networks and of model systems constructed to approximate fat-crystal networks has been the focus of much endeavor since the early 1960s [2–9]. However, most of these models failed to adequately describe the fat-crystal network quantitatively. In all cases, this was due to the failure of the network models to describe the fractal nature of the network [10,11]. Until now there has been no incorporation of the fractal arrangement, at certain length scales, of the network into structural models.

Any attempt to quantitatively relate aspects of network structure to rheological properties must necessarily examine the different levels of structure present in the network, and the contribution of these levels of structure to various rheological indicators, such as yield stress and storage modulus. The fats industry has long accepted the yield value of the network as a rheological indicator of the hardness of the network. Furthermore, methods developed as early as 1959 by Haighton [12] related cone penetrometry measurements to the sensory hardness of fats, and established an empirical formula to determine yield value from such measurements. However, Shama and Sherman [13] pointed out that the yield value as related to cone penetrometry does not necessarily relate to any fundamental properties of the crystal network, since the large shearing forces involved in cone penetrometry measurements results in drastic damage to the network structure. Soon after, Davis suggested that linear viscoelastic testing or small-deformation measurements (such as the elastic modulus of the network) performed on the fat-crystal network should yield more information on the intact structure of the network [14]. Furthermore, measurements in our laboratory indicate that there exists a direct relationship between the elastic modulus (storage shear modulus) of a fat and its hardness index, as determined by cone penetrometry measurements [15]. Therefore, the elastic modulus of a fat-crystal network is an indicator of the macroscopic consistency of that network which also allows one to observe contributions from the undamaged network structure. In the model we propose, the rheological indicator of importance is the elastic modulus.

The structure of fat-crystal networks is arranged in a hierarchical fashion, with combinations of different levels being implicated in varying degrees depending on the nature of the rheological measurement. The growth of a fat-crystal network can be visualized thus: the triglycerides present in the sample crystallize from the melt into particular polymorphic-polytypic states. These crystals grow into larger microstructural elements ($\sim 6\ \mu$m) which then aggregate via a mass- and heat-transfer limited process into larger microstructures ($\sim 100\ \mu$m). The aggregation process continues until a continuous three-dimensional network is formed by the collection of microstructures. Trapped within this solid network structure is the liquid phase of the fat. As shown by Narine and Marangoni [11], the microstructural elements are arranged in a fractal manner within the microstructures.

Since the quantification of the spatial distribution of the microstructural elements within microstructures of fats was achieved early this year via fractal analysis [11], methods are now available to quantify all levels of structure in fat-crystal networks. For the smallest scale of structure present, the tri-

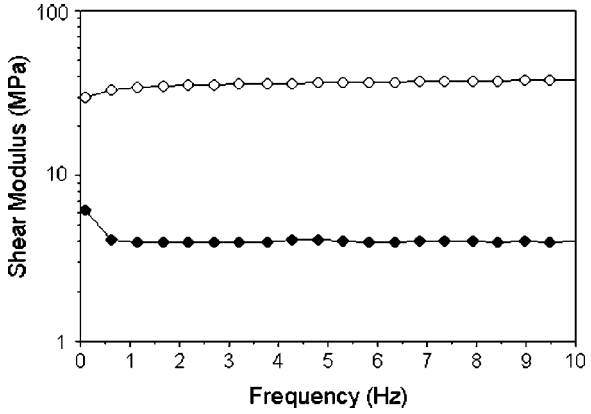

FIG. 1. Shear elastic modulus G'(○-○) and loss modulus G''(●-●) plotted against frequency for cocoa butter (solid fat content of sample is 75% and strain level is 0.5%).

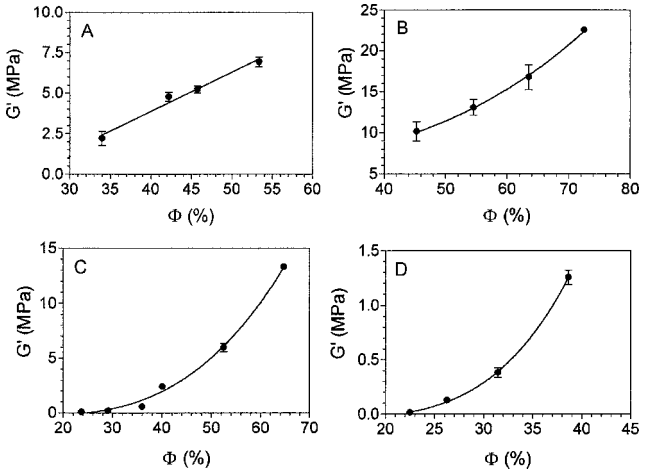

FIG. 2. Shear elastic modulus G' plotted against volume fraction of solid fat Φ for (a) milkfat, (b) tallow, (c) palm oil, and (d) lard (strain levels used are 0.2%).

glyceride molecules, methods to determine triglyceride and fatty acid composition as well as stereo-specific structural analysis are well established [16]. The different polymorphic and polytypic states formed by the crystallizing triglycerides have been quantified by powder x-ray-diffraction (e.g., [17,18]), Fourier transform infrared analysis (e.g., [19,20]) and differential scanning calorimetry measurements (e.g., [21]). Furthermore, methods to quantify solid and/or liquid ratios of fat-crystal networks are also available (e.g., [22–25]). However, although all structural levels of the network can be quantified as well as the solid and/or liquid ratios, there is still no conclusive theory to relate triglyceride composition, crystal orientation, crystal size, crystal shape, microstructural characteristics, and solid fat content to the elastic modulus of the fat network. A quantitative network model incorporating the various levels of structure in the appropriate degrees depending on the extent to which they affect the elastic modulus of the network is therefore even more important than before, given that the different structural levels can all be quantified.

The elastic modulus of fat-crystal networks are virtually independent of frequency and in the linear viscoelastic region demonstrate a very low value of damping [3,15]. An example of the lack of variation of the elastic modulus with frequency is shown in Fig. 1 (experimental details are summarized in Sec. III below). This suggests that the viscosity of the liquid (oil) portion of the network plays no essential part in the transmittance of forces; if this was the case, one would expect increases of the loss modulus with increases in frequency [3]. The fact that fat-crystal networks do demonstrate a measurable elastic modulus as well as a yield value suggests that the solid fat particles are the entities responsible for the elastic modulus and therefore these particles must have strong mutual interactions.

The quantification of the spatial distribution of microstructural elements within the microstructures in fat-crystal networks has been studied using the relationship of the shear elastic modulus (G') to the volume fraction of solid fat (Φ) via the mass fractal dimension (D) of the network [11]. This work closely paralleled advances in application of scaling theory to explain the elastic properties of colloidal gels [26–35] developed after introduction of the fractal concept by Mandelbrot [36]. The elastic modulus of a fat-crystal network is related to the solid fat content of the network via the following relationship at high solid fat contents (~60–100 %):

$$G' = \gamma \Phi^{1/(d-D)}, \tag{1}$$

where G' is the elastic modulus, γ is a constant which is dependent on the size of the primary particles and on the interactions between them, Φ is the particle volume fraction of solid fat, d is the Euclidean dimension of the network—usually 3—and D is the fractal dimension of the network, measured at length scales bounded by the average size of the microstructural elements and the size of one microstructure. The exact dependence of the constant γ on network properties has not been formulated: it is the motivation of the model outlined in this publication to formulate a relationship of γ to fundamental characteristics of the fat network in a manner that would render γ quantifiable and therefore allow Eq. (1) to be used as a tool to predict the elastic modulus of a particular fat-crystal network with a known solid fat content. One of the reasons previous models of fat-crystal networks failed was that they predicted a linear relationship between the elastic modulus and the solid fat content of the network. As shown by Eq. (1) and as verified by a host of researchers (e.g., [3–6,10,11,36,37]) the elastic modulus of the network actually depends on the solid fat content in a power law fashion. Figure 2 shows a plot of G' vs Φ for four different systems (experimental details are summarized in Sec. III below). For Fig. 2(a) the fat system demonstrated is milkfat; the relationship is linear because the fractal dimension D of milkfat is 2.02 [11], therefore, from Eq. (1), the G' dependence of Φ is linear.

II. THEORY

At the microstructural level, the solid network is an orthodox amorphous solid, while the intramicrostructural level is fractal in nature [11]. In this way, the formation of the fat-crystal network is mathematically very similar to a flocculating colloid as noted by Edwards and Oakeshott [39]. The arrangement of the microstructures can be imagined as an assembly of chains, each chain consisting of a linear array of

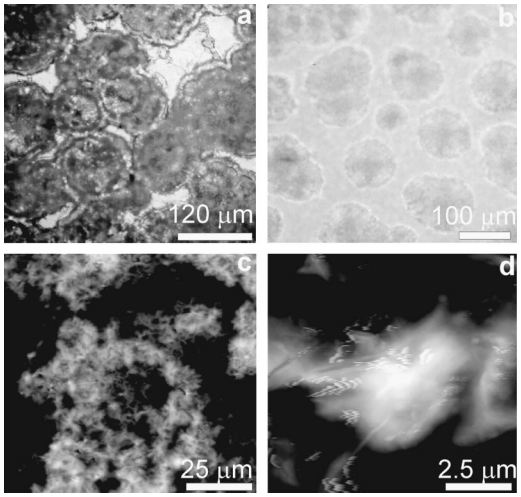

FIG. 3. (a) Microstructures of cocoa butter. (b) Microstructures of milkfat. (c) Microstructure of the high melting fraction of milkfat. (d) Microstructural element of the high melting fraction of milkfat. (a) and (b) were imaged with a polarized light microscope and the fat was dispersed in 50% (w/w) canola oil, (c) and (d) were imaged with an atomic-force microscope.

microstructures with an average small mutual distance apart. The chains are branched and interlinked to form a three-dimensional network with oil present in the void volume, both within and without the microstructures. In this way the network is similar to the network as described by van den Tempel [2]. However, van den Tempel did not consider that the particles forming the chains were clusters of smaller particles arranged in a fractal manner; the way the microstructures are clusters with microstructural elements arranged within them in a fractal manner. In a later publication, van den Tempel did consider that the network is formed via interaction of clusters rather than primary particles [7], but did not consider the fractal arrangement of the ''primary particles'' within the clusters. Evidence of the existence of ordered microstructures is given by Heertje and co-workers [40–42] as well as Narine and Marangoni [11]. The fractal nature of the microstructures was demonstrated by Narine and Marangoni [11]. Figures 3(a) and 3(b) show microstructures of cocoa butter and milkfat, as seen under a polarized light microscope. The fractal arrangement of microstructural elements in fat crystals was demonstrated in Ref. [11]. Figures 3(c) and 3(d) show a microstructure and microstructural element of the high melting fraction of milkfat seen under an atomic-force microscope operated in tapping mode (experimental details are summarized in Sec. III below).

A. Weak-link theory

The relationship shown by Eq. (1) was formulated by assuming the so called ''weak-link theory'' in which the elastic constant of the network is dependent on the nature of the links between microstructures, as opposed to the strength of the microstructures themselves [11,34]. This theory is only applicable to fat-crystal networks at relatively high percentages of solid content (~60–100 %). The weak-link theory suggests that when a deforming force is placed on the fat-crystal network such that the resulting deformation is within the linear viscoelastic region of the network, the links between the microstructures are stressed, rather than the microstructures themselves. Figure 4 is a schematic depicting an idealized fat-crystal network under shear. Some experimental evidence of the weak-link theory is provided in a paper by Heertje [42]. This paper showed a fat network in an unstressed and stressed state; in the stressed state, the microstructures are separated with respect to each other, but have maintained their shape and size. This would seem to suggest that the weakest link in the network occur at the link between microstructures. Further proof of the weak-link theory is offered in the publication by Narine and Marangoni [11], where microscopic and rheological determinations of fractal dimensions of a series of fat-crystal networks were seen to agree within 2.5%, using the weak-link theory and Eq. (1).

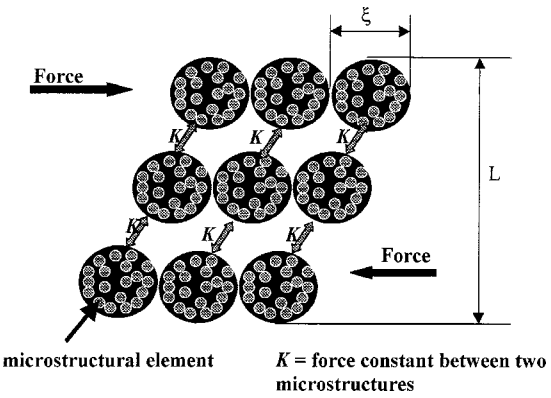

FIG. 4. Schematic of idealized fat-crystal network under shear.

B. Fractal network model

In a 1 cm^3 sample containing N_ξ microstructures, with N_σ microstructural elements in each microstructure, the solid fat content of the network is given by

$$\Phi = \frac{4}{3}\pi\left(\frac{\sigma}{2}\right)^3 N_\sigma N_\xi, \tag{2}$$

where σ is the diameter of a microstructural element assumed to be spherical. This assumption is not a bad assumption for most natural fat systems at high solid fat contents as the authors have observed with polarized light microscopy. The number of microstructural elements within a microstructure is given by the following equation [35,43]:

$$N_\sigma \sim \left(\frac{\xi}{\sigma}\right)^D \tag{3}$$

$$\Rightarrow N_\sigma = c(\xi)^D, \tag{4a}$$

where ξ is the diameter of a microstructure and c is proportionality constant. As explained by Narine and Marangoni [11], the fractal dimension of a fat-crystal network may be calculated by utilizing Eq. (4a) in the following form:

$$N_\sigma = c(R)^D, \tag{4b}$$

where $\sigma \leqslant R \leqslant \xi$. Taking logarithms

$$\ln(N_\sigma) = D\ln(R) + \ln(c). \tag{5}$$

Therefore, a plot of $\ln(N_\sigma)$ vs $\ln(R)$ yields $\ln(c)$ as the intercept and D as the slope. Therefore, from Eq. (2),

$$\Phi = \frac{4}{3}\pi\left(\frac{\sigma}{2}\right)^3 c(\xi)^D N_\xi. \tag{6}$$

The number of microstructures in a sample of volume 1 cm^3 may therefore be written as

$$N_\xi = \frac{6\Phi}{c\pi\sigma^3\xi^D}. \tag{7}$$

If the mutual distance between neighboring microstructures in a chain is small compared to ξ, the total length of all the chains present in the 1 cm^3 sample is

$$N_\xi \xi = \frac{6\Phi\xi}{c\pi\sigma^3\xi^D}. \tag{8}$$

We can safely assume that the total chain length is made up of straight chains oriented in three mutually perpendicular directions in a cubic sample, given the regular manner in which the microstructures have been observed to pack [40–42]. Therefore, when the network is stressed in a given direction only one third of the total chain length represents the number of chains supporting stress in that direction. In a cube of volume 1 cm^3, a cross section of area 1 cm$\times$1 cm cuts through the following number of 1 cm chains:

$$\frac{N_\xi \xi}{3} = \frac{2\Phi\xi^{1-D}}{c\pi\sigma^3}. \tag{9}$$

These are, therefore, the chains that transmit stress from one part of the sample to the other.

C. Forces acting within the network

We assume that the attractive forces between microstructures consist of van der Waals interactions between microstructural elements that form nearest neighbors at the interface between two microstructures. One can imagine that if the microstructures all are of the same size and shape, there will be some m interactions due to nearest-neighbor interactions between microstructural elements at the edge of two neighboring microstructures. Therefore, as far as the elastic modulus of the network constitutes a measure of the mechanical strength of the network at small deformations, all of the microstructural elements present do not contribute to the mechanical strength. The relatively few microstructural elements that link the microstructures together are moved with respect to their nearest neighbors in a neighboring microstructure when the network is stressed, while the microstructures themselves behave as rigid units. This view of the behavior of the network under a deforming stress is shared by Papenhuijzen [6]. The assumption that van der Waals interactions are the interactions of importance with fat particles is not new [2–4] and as Nederveen [3] has stated, it may be calculated that dipolar forces are about a factor of 10^{10} smaller than van der Waals forces, making these negligible enough to ignore. Furthermore, the fat particles are nonpolar and the oil is a nonpolar medium.

It is difficult to take into consideration nonspherical shapes in a calculation of van der Waals' forces, although this has been attempted before [44]. Therefore, in the following development, the microstructural elements are assumed to be spherical, a reasonable assumption as explained above. Below, we summarize a development of the calculation of van der Waals interaction between two microstructural elements, developed by Nederveen [3]. The Lennard-Jones potential between two nonpolar atoms is formulated as

$$U = -\lambda r^{-6} + \mu r^{-12}, \tag{10a}$$

$$\lambda = 2|U_0| r_0^6, \tag{10b}$$

$$\mu = \frac{\lambda}{2} r_0^6, \tag{10c}$$

where U is the potential energy of two molecules at a distance r. When the two molecules are at their equilibrium distance r_0 apart, the potential energy is U_0. In order to calculate the attractive energy between two spheres consisting of a large number of molecules (say, q/m^3), Eq. 10(a) must be integrated over the volumes of both spheres:

$$U = q^2 \int_{\nu_1} d\nu_1 \int_{\nu_2} d\nu_2 (-\lambda r^{-6} + \mu r^{-12}). \tag{11}$$

where $d\nu_1$, $d\nu_2$, V_1, and V_2 are volume elements and volumes of the 2 spheres 1 and 2 and r is the distance between $d\nu_1$ and $d\nu_2$. Hamaker [45] had before Nederveen carried out the integration of the attractive term. By carrying out the integration for the repulsive term as well, it is possible to calculate the stiffness of a van der Waals bond for small deviations from equilibrium, such as is the case when the network is deformed during measurement of the elastic modulus. Nederveen performed the integration for two spheres with equal radii R separated by a distance d (making the distance between the centers of the two spheres $C = 2R + d$). The steps of the integration are cumbersome and unnecessary to restate at this point. It is sufficient to say that for $d \ll R$ (see Ref. [3]). Nederveen's integration agreed with an independent check by the authors and yielded

$$U = \frac{-AR}{12d}\left[1 - \frac{1}{420}\left(\frac{r_0}{d}\right)^6\right], \tag{12}$$

where $A = \pi^2 q^2 \lambda$ is the Hamaker's constant. The attractive force between the two spheres is given by differentiation of Eq. (12) with respect to d:

$$F = \frac{\partial U}{\partial d} = \frac{AR}{12d^2}\left[1 - \frac{1}{60}\left(\frac{r_0}{d}\right)^6\right]. \tag{13}$$

Equations (12) and (13) suggest that there is an equilibrium distance where the potential energy between the two spheres is a minimum and the force between them becomes zero:

$$d_0 = \frac{r_0}{\sqrt[6]{60}}. \tag{14}$$

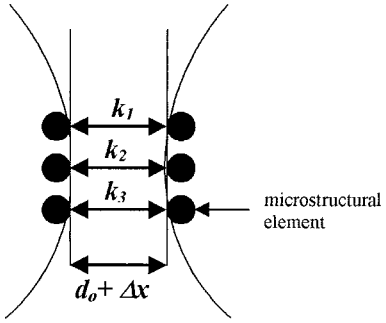

FIG. 5. Schematic showing forces between two microstructures.

'If the deformation ε of all volume elements in the two spheres is homogenous, then d may be written as a function of the radius of the spheres:

$$d = d_0 + 2R\varepsilon. \tag{15}$$

When Eqs. (14) and (15) are substituted into Eq. (13):

$$F = \frac{AR^2\varepsilon}{d_0^3}\left(1 - \frac{11R\varepsilon}{d_0}\right). \tag{16}$$

This equation is valid only when $11R\varepsilon/d_0$ is small compared to unity. Therefore, for very small deformations, the force between the two spheres varies linearly with the deformation.

It is expected that as two microstructural elements move apart due to a stress on the network, the resulting gap is filled with the liquid oil present in these networks. Papenhuijzen [6] has shown that by considering the microstructural elements as spheres and using a corrected Stokes equation:

$$f_h = 3\pi\eta_L R u \alpha, \tag{17}$$

where f_h is the force necessary to move a sphere with diameter R at speed u to a flat plate, n_L is the viscosity of the oil, and α is a correction factor which depends on the distance between the sphere and the plate, the corresponding hydrodynamic force can be expressed as

$$f_h = \frac{3\pi\eta_L R^2 u}{8d}. \tag{18}$$

As reported by Kamphuis and Jongschaap [9], the elongation rate between the two spheres is assumed to be very small:

$$u \ll \frac{A}{\eta_L R d}, \tag{19}$$

and therefore only the Lennard-Jones potential as described above needs to be taken into account. These authors also suggested that the inertial forces are negligible with respect to the interactive forces [8]. This is assumed as well in our treatment.

Figure 5 shows a schematic of two neighboring microstructures. The force between two neighboring microstructural elements is given by Eq. (16). If the microstructural elements are assumed to be identical, the interaction between neighboring microstructural elements can be represented by a spring. Therefore, the forces between microstructures can be represented as m identical springs of spring constant k in parallel. If one assumes that the pairs of microstructural elements are all moved the same distance apart, then the total force can be approximated by

$$F = \sum_1^m k_n \Delta x = \sum_1^m f_n = mf, \tag{20}$$

where f is the restoring force of one spring of force constant k extended by a distance of Δx. Therefore, if there are m identical pairs of microstructural elements at the interface between two microstructures, the force between the microstructures is given by

$$F = m\frac{A\sigma^2\varepsilon}{4d_0^3}\left(1 - \frac{11\sigma\varepsilon}{2d_0}\right), \tag{21}$$

where R in Eq. (16) has been replaced by $\sigma/2$ to represent the radius of the microstructural elements.

D. Elastic modulus

In a sample that is a cube of volume 1 cm^3 which is stressed in one direction, the number of chains carrying the stress is given by Eq. (9). Therefore, the stress s transmitted through a 1 cm$\times$1 cm cross section is given by [2,3,9]

$$s = m\frac{A\sigma^2\varepsilon}{4d_0^3}\frac{2\Phi\xi^{1-D}}{c\pi\sigma^3}\left(1 - \frac{11\sigma\varepsilon}{2d_0}\right)$$
$$= m\varepsilon\frac{A\Phi\xi^{1-D}}{2c\pi\sigma d_0^3}\left(1 - \frac{11\sigma\varepsilon}{2d_0}\right). \tag{22}$$

The tensile modulus of the network is then given by

$$E = \frac{s}{\varepsilon} = m\frac{A\Phi\xi^{1-D}}{2c\pi\sigma d_0^3}\left(1 - \frac{11\sigma\varepsilon}{2d_0}\right). \tag{23a}$$

When the deformation is small enough that one is in the linear viscoelastic region and the following relationship holds:

$$\frac{11}{2}\frac{\sigma\varepsilon}{d_0} < 0.1, \tag{23b}$$

Eq. (23a) reduces to

$$E = \frac{s}{\varepsilon} = m\frac{A\Phi\xi^{1-D}}{2c\pi\sigma d_0^3}. \tag{24}$$

The storage shear modulus is given by

$$G = \frac{E}{3} = m\frac{A\Phi\xi^{1-D}}{6c\pi\sigma d_0^3} = m\frac{A\Phi\xi^{2-D}}{6c\pi\sigma\xi d_0^3}. \tag{25}$$

If the fractal dimension within microstructures is D, i.e., the spatial distribution of the microstructural elements within the microstructures is characterized by D, the scaling relationship between the average microstructural size ξ and the solid volume fraction Φ can be found by approximating the solid volume fraction inside the microstructures as the overall solid volume fraction:

$$\xi \sim \Phi^{1/(D-d)}. \tag{26}$$

This relationship is well known in semidilute polymer solutions [46] and was shown by Dietler *et al.* [47] to be correct for colloidal silica gels as well. Furthermore, this relationship was seen to be supported for fat-crystal networks [11]. From Eq. (26),

$$\xi^{2-D} \sim [\Phi^{1/(D-d)}]^{2-D} = \Phi^{(2-D)/(D-d)}. \tag{27}$$

Therefore,

$$\Phi \xi^{2-D} \sim \Phi \Phi^{(2-D)/(D-d)} = \Phi^{(d-2)/(d-D)}. \tag{28}$$

From the above,

$$G' \sim m \frac{A}{6c\pi\sigma\xi d_0^3} \Phi^{(d-2)/(d-D)} = m \frac{A}{6c\pi\sigma\xi d_0^3} \Phi^{(1/d-D)}. \tag{29}$$

Equation (29) therefore reduces to a form equivalent to Eq. (1):

$$G' \sim \frac{mA}{6c\pi\sigma\xi d_0^3} \Phi^{1/(d-D)}. \tag{30}$$

Comparing Eq. (1) and Eq. (30),

$$\gamma \sim \frac{mA}{6c\pi\sigma\xi d_0^3}. \tag{31}$$

Throughout the above treatment, particle volume fraction and solid fat content (Φ) has been used interchangeably. The relationship between these quantities is: particle volume fraction=(density of network/density of microstructural elements)Φ.

III. EXPERIMENTS

A. Rheology

Rheological analysis of all the fat systems was performed as detailed below. All rheological measurements were made using a CarriMed CSL^2 500 Rheometer (TA Instruments) with a 2-cm parallel plate attachment. Rheological analysis of cocoa butter was performed at 20 °C, and all other systems were analyzed at 5 °C; to facilitate the variable and low temperatures used, one of the attachment plates of the instrument is a Peltier plate. Liquefied blends of the fats were poured into molds in order to ensure uniformity in thickness and diameters—the diameter of the resulting samples are the same as the attachment plates on the CarriMed instrument and the thickness of the samples were 3.2 mm. The fats were allowed to crystallize in the mold at 5 °C for 48 h (except for cocoa butter, where the molds were cooled at 5 °C for 1 h and then incubated at 20 °C for 48 h). To prevent slippage between the sample surface and the surface of the attachment plates on the CarriMed, 50 grit sandpaper was attached to both attachment plates with Krazy Glue™ (for cocoa butter, Krazy Glue™ was used to attach the sample to the attachment plates without any sandpaper).

After the sample was mounted in the manner described above, the rheometer was run through an oscillatory stress program (applied stresses ranging from 1 to 31 800 Pa at a frequency of 1 Hz). This stress program is initially performed on one replicate of the sample in order to determine the linear viscoelastic region (LVR). On establishment of the LVR, frequency sweeps of the data were carried out at constant strains (0.5%) over a frequency range of 0.1–10 Hz. Figure 1 shows such a frequency sweep for cocoa butter at 75% solid fat content. Additionally, measurements of G' were made in the LVR by applying a variable stress program to replicates of the sample, and reading G' at strain levels of 0.2% (well within the LVR for these materials). Figure 2 shows values of G' plotted against different values of solid fat content for various fat systems.

The ln of the obtained values of G' and Φ were plotted against each other, and the slope of the line was determined by linear regression. This has been described in Ref. [11]. Assuming a weak-link regime, the slope of this line is given by $1/(3-D)$, and therefore the fractal dimension of the particular fat system can be calculated based on the rheological measurement.

B. Solid fat content

Solid fat content was determined with a Bruker PC/20 series NMR Analyzer (Bruker, Milton, ON, Canada). Different solid fat contents were achieved for each fat system using canola oil as a diluent for milkfat, lard, cocoa butter, and tallow samples, while soyabean oil was used as a diluent for palm oil samples. The blends were introduced into NMR tubes, and allowed to crystallize using the same temperature regimes under which the rheological samples were crystallized.

C. Polarized light microscopy

Solid samples of milkfat, cocoa butter, and tallow were prepared by dilution with 50% canola oil, and then heated to 80 °C. A small droplet of the melted fat was then placed on a glass slide and smeared into a thin film by holding the slide vertically. The fat was then allowed to crystallize at the desired temperature for 48 h and then imaged under a polarized light microscope (PLM) at low magnification. This allowed the microstructures of the system to be seen. However, because of the large amount of dilution, resulting in low values of solid fat content, the microstructures themselves did not form a solid network, but in effect were ''floated'' away from each other in the oil. This facilitates the imaging of the microstructures, which in an *in situ* PLM image are difficult to discern.

Samples of milkfat-canola, cocoa butter-canola, lard-canonla. and tallow-canola (in 85% w/w fat system-canola oil), palm oil-soyabean oil (85% w/w palm oil soyabean oil) blends were analyzed using polarized light microscopy. The samples were prepared by melting the prepared blends of the fat systems at 80 °C, and using a Pasteur pipette to deposit a small droplet of fat onto a glass slide preheated to the temperature of the melted fat. A similarly heated glass coverslip was then dropped onto the surface of the droplet, ensuring that the plane of the coverslip was parallel to the plane of the slide. This allowed the droplet to be smeared out into an extremely thin rectangular block of fat of uniform thickness. The samples were then allowed to crystallize for 48 h at the

desired temperature. When imaged under a PLM at high magnification, the microstructural elements of the network can be visualized. This procedure is also described in Ref. [11], and images so taken are shown in this reference.

In an alternate method, noninteresterified lard and chemically interesterified lard were crystallized under identical crystallization conditions and a small amount of fat was placed on a glass slide. A drop of paraffin oil was then added as a dispersing aid. A cover slip was then firmly pressed on the sample to remove air bubbles and excess liquid. This process breaks the network in such a manner as to allow the imaging of dispersed microstructural elements with a polarized light microscope. This method was used as a way of determining effective diameters of microstructural elements of lard and chemically interesterified lard.

D. Fractal dimensions

As described in Ref. [11], mass fractal dimensions can be calculated from the images of the microstructural elements of the different fat systems. It should be noted here that mass fractal dimensions of samples of the same fat system at different values of high solid fat content (60–100%) were the same. Mass fractal dimensions have been calculated in Ref. [11], and the values so calculated may be then compared to the rheologically determined mass fractal dimension.

E. Measuring effective values of σ and ξ

The diameters of the microstructural elements of the fat systems that can be measured using the *in situ* polarized light microscope images of fat systems that have been diluted with 15% by weight canola oil (soyabean oil in the case of palm) are not necessarily an absolute measure of these diameters. However, PLM images of these entities does allow an ''effective'' diameter to be measured, which may then be used to demonstrate the dependence of G' on these parameters. A PLM image of microstructural elements contains those elements both in focus as well as those elements out of focus. An attempt was made to select those microstructural elements that are obviously in focus to be measured for values of σ. For measurement of the diameter of microstructures, attempts were made to measure only those elements with an obviously repeating size, i.e., effort was made to ignore those clusters of fat which seemed to be composed of more than one microstructure.

F. Atomic-force microscopy

Samples of the high melting fraction of milkfat were imaged using an atomic-force microscope. Samples of the fat were melted at 80 °C and then a small droplet was dropped onto a polished silicon (111) surface, which was rotating at a speed of 4000 rpm. The droplet was thus spin-coated on the silicon for 90 s. The resulting thin coating of fat on the silicon wafer was then incubated at 20 °C for 24 h. The resulting fat surface was then imaged using a Nanoscope IIIa atomic-force microscope (Digital Instruments) operated in tapping mode with the cantilever being driven at 250 kHz. The cantilever used in this case had a force constant in the range 40–85 N/m.

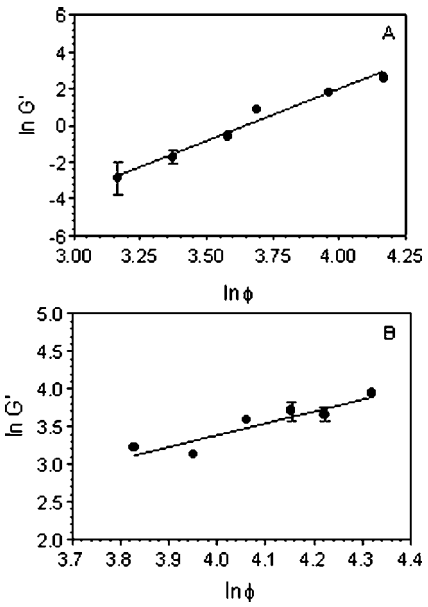

FIG. 6. $\ln G'$ vs $\ln \Phi$ for (a) palm oil and (b) cocoa butter.

IV. RESULTS

Figure 1 shows a plot of shear elastic modulus and loss modulus plotted against frequency for a 75% solid fat content sample of cocoa butter. The strain level used here was 0.5%.

Figure 2 shows the shear elastic modulus G' plotted against solid fat content for milkfat, tallow, palm oil, and lard. The shear elastic modulus was measured at strain levels of 0.2%.

Figures 3(a) and 3(b) show microstructures of cocoa butter, and milkfat, respectively. The fats were first blended with 50% w/w of canola oil, to facilitate the discernment of the microstructures. The microstructures here are somewhat displaced from their regular packing arrangement, since the system is dilute enough so that the microstructures are dispersed in the oil. Figures 3(c) and 3(d) show atomic-force images of a microstructure and microstructural element, respectively, of the high melting fraction of milkfat.

As have been shown in Ref. [11], Eq. (1) accurately describes the behavior of fat-crystal networks. Equation (30) is of the same form as Eq. (1), with Eq. (31) showing that the pre-exponential terms in Eq. (1) may be represented by the constant γ. The ln of measured values of G' and Φ were plotted against each other for different fat systems. Figures 6(a) and 6(b) show $\ln G'$ vs $\ln \Phi$ for palm oil and cocoa

TABLE I. Fractal dimension calculated via image analysis compared to fractal dimension calculated via rheology using the weak-link theory of Shih *et al.* [34]. Errors in D are standard errors of three replicates.

Fat system	Fractal dimension from image analysis	Fractal dimension from rheology (weak-link regime)	Percent deviation
Cocoa butter 1	2.31±1.7%	2.37±4.0%	2.5
Palm oil	2.82±0.6%	2.82±0.6%	0.0

butter, respectively. From the slope of such lines, the fractal dimension may be determined, as is explained in the experimental section above. The fractal dimension of the different fat systems may also be determined by analysis of the PLM images of the microstructural elements of the fat systems, as is explained in Ref. [11]. Table I show a comparison between fractal dimensions determined for palm oil and cocoa butter from rheology and from image analysis (this comparison was also reported in Ref. [11] together with three other fat systems).

Figure 7 shows a plot of values of G' vs $1/\sigma$, where σ is a measure of effective diameters of microstructural elements for five different fat systems. Figure 8 shows a plot of values of G' vs $1/c\sigma\xi$ for three different fat systems. Values of the constant γ were calculated from the intercept of the $\ln G'$ vs $\ln\Phi$ plots of the rheological data collected for each of the five fat systems. Values of G' used in Figs. 7 and 8 were calculated using the rheologically determined values of γ, the mass fractal dimension, Eq. (1) and a common value for the solid fat content ($\Phi = 70\%$). A common value for the solid fat content was used in order to effectively normalize the value of G' with respect to solid fat content, thereby allowing a better comparison to other parameters such as σ, c, and ξ.

Figures 9(a) and 9(b), respectively, show polarized light microscope images of 70% w/w samples of noninteresterified lard/canola oil and chemically interesterified lard/canola oil. These samples were imaged using the method of dispersion with paraffin oil described in the experimental section. The shear elastic moduli corresponding to these samples are 1.25×10^4 Pa and 3.34×10^5 Pa, respectively. As is evidenced by the sizes of the microstructural elements represented in the pictures, the fat with the smaller microstructural elements (chemically interesterified lard/canola oil) has a larger value of shear elastic modulus.

V. DISCUSSION

It is important to note that the power-law relationship between G' and Φ of Eqs. (1) and (30) is only valid for deformations of the fat network small enough such that Eq. (23b) holds. Additionally, Eq. (30) has been manipulated to represent the same functional form as Eq. (1). As a result, the average diameter of the microstructures in the network ξ appears in the denominator of Eq. (31). However, according to Eq. (26), ξ is related to the solid volume fraction. It is important to realize that Eqs. (1), (30), and (31) are only valid at high solid fat contents. It has been experimentally proven that at high solid fat contents (~60–100 %), the constant γ is independent of the solid fat content; plots of $\log_{10} G'$ vs $\log_{10}\Phi$ of some eight different fat systems were statistically good straight lines with a measurable intercept corresponding to $\log_{10}\gamma$ [11]. This, therefore, would suggest that ξ as it appears in the denominator of Eqs. (30) and (31) does not change significantly over the applicable range of solid fat content. Furthermore, the authors have observed no measurable change in the diameter of microstructures of cocoa butter observed in its natural state at 20 °C and at dilutions of 5, 10, 15, 20, 25, and 30 % w/w with canola oil. The canola oil

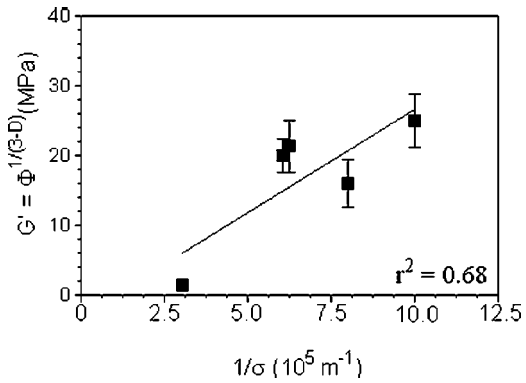

FIG. 7. Plot of G' vs $1/\sigma$ for five different fat systems. Symbols with error bars represent average values of rheological measurements and their standard deviations.

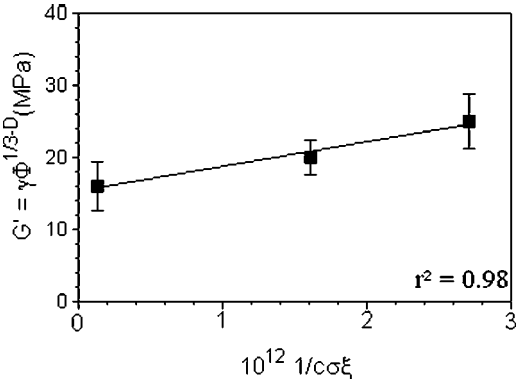

FIG. 8. Plot of values of G' vs $1/c\sigma\xi$ for three different fat systems. Symbols with error bars represent average values of rheological measurements and their standard deviations.

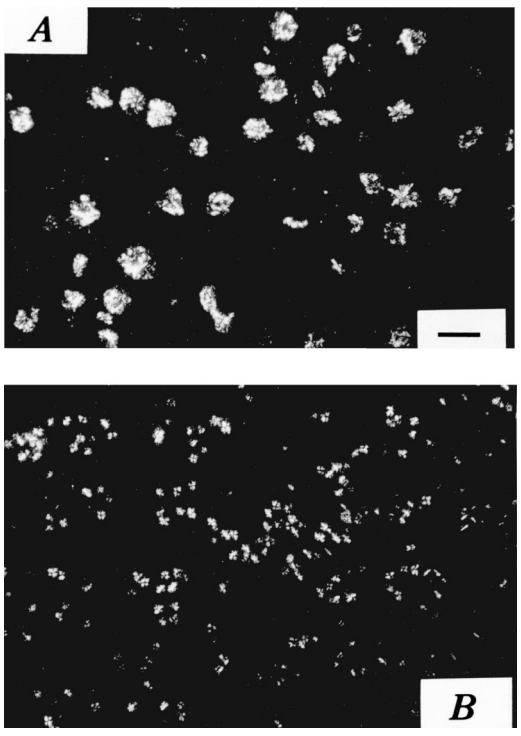

FIG. 9. Polarized light microscope images of (a) 70% w/w samples of noninteresterified lard/canola oil and (b) chemically interesterified lard/canola oil. These samples were imaged using the method of dispersion with paraffin oil.

in this case was used purely as a diluent to vary the solid fat content.

The dependence of the hardness of fats on the solid fat content has been studied by a variety of researchers (e.g., [1,3,10,11,37,38,48,49]). In all cases hardness depended on the solid fat content in a power-law fashion. This is supported by Eq. (30). Furthermore, as is demonstrated by Fig. 6, a plot of $\ln G'$ vs $\ln \Phi$ yields a straight line, verifying the power-law dependence of G' on Φ. Additionally, as have already been shown in Ref. [11], Table I shows that rheologically calculated values of fractal dimension agree well with fractal dimensions calculated from image analysis. This suggests that both Eqs. (1) and (30) are correct in their description of fat-crystal networks, as far as variation of G' with Φ and D is described by the model.

Particle size has been shown experimentally to be an important parameter in the hardness of fat-crystal networks (e.g., [1,3,13,49–56]) but previous network models except for Refs. [2,7], failed to show a dependence on particle size in the final expression for the shear elastic modulus [3–6,8,9]. Overwhelming experimental evidence has been submitted by other researchers [50–56] which demonstrates that the hardness of fat-crystal networks is inversely proportional to the particle size (microstructural element size). This is also supported by Eq. (30). Equation (30) demonstrates a dependence on both the size of the microstructures and the size of the microstructural elements. As is demonstrated by Fig. 7, a plot of G' vs $1/\sigma$ yields a proportional relationship, as is predicted by Eqs. (30) and (31), and as have been shown before by a host of other researchers [50–56]. The fit to a straight line yields an r^2 value of 0.68. The fit is significantly improved when G' is plotted versus $1/c\sigma\xi$ as is seen in Fig. 8, the r^2 value here being 0.98. This relationship is again predicted by Eqs. (30) and (31). The fact that the straight line fit to the plot of G' versus $1/c\sigma\xi$ is better than the plot of G' vs $1/\sigma$ is important to note, since it seems that changes in σ are followed by changes in both c and ξ. It is not surprising that these parameters are covariants, since from Eqs. (3) and (4a), the parameter c is a measure of how many microstructural elements of a particular diameter σ are contained in a microstructure of a particular diameter ξ for that particular fat with a particular value for the fractal dimension D. Obviously, changes in ξ and σ also affects the value of c. Consequently, a better analysis of the agreement of the model with such parameters as c, σ, and ξ is provided by evaluating the effect of these parameters on G' collectively rather than individually. We have been unable to procure measurements of m, d_0, and A at this time.

As a visual example of the effect a decrease in microstructural element size has on the shear elastic modulus, Fig. 9 shows marked decrease in particle size from the sample of noninteresterified lard and/or canola oil to the sample of chemically interesterified lard and/or canola oil. There is a corresponding increase in the shear elastic modulus as well, the shear elastic modulus increases from 1.25×10^4 Pa to 3.34×10^5 Pa, as would be expected from the decrease in the diameter of the microstructural elements shown dispersed in the images.

The morphology of the microstructural elements also affects the mechanical strength of the network (e.g., [57–59]). Since the interactions between the microstructural elements in this model were developed for spherical microstructural elements, obviously morphological changes of these elements would vary the form of Eq. (30). Additionally, changes in morphology would probably cause changes in the Hamaker's constant as well. Morphology and size of crystals are affected by the particular polymorphism of the fat crystals formed [17,59]. The triglyceride composition also influences the size and rigidity of the crystals [1]. Therefore, it is important to establish a relationship between Hamaker's constant and triglyceride composition and polymorphism.

VI. CONCLUSION

While Eq. (30) does not provide an absolute formulation for γ in Eq. (1), it does identify key network parameters that are important in determining the shear elastic modulus of fat-crystal networks. Furthermore, it agrees well with experimental observations and with Eq. (1), which has been shown [11] to be valid for fat-crystal networks. The equation provides impetus for the development of phenomenological investigations of relationships between triglyceride composition and polymorphism and values of Hamaker's constants and size of microstructural elements. Insight on the changes in mechanical strength of fat networks whose characteristics, such as size of microstructural elements, size of microstructures, and distances between microstructures, have been altered through processing conditions, is also provided.

ACKNOWLEDGMENTS

The authors thank Rekha Narine for proofreading the manuscript, Professors Robert Lencki and Alan J. Slavin for discussions concerning the model, and the Natural Sciences and Engineering Research Council of Canada (NSERC) for financial support. The help of Professor Peter Norton, Claire McCague, and Joy Munro, of the University of Western Ontario, with the imaging of fats using atomic-force microscopy is gratefully acknowledged.

[1] A. E. Bailey, *Melting and Solidification of Fats* (Interscience, New York, 1950).
[2] M. van den Tempel, J. Colloid Interface Sci. **16**, 284 (1961).
[3] C. J. Nederveen, J. Colloid Interface Sci. **18**, 276 (1963).
[4] A. R. Payne, J. Colloid Interface Sci. **19**, 744 (1964).
[5] J. M. P. Papenhuijzen, Rheol. Acta **10**, 493 (1971).
[6] J. M. P. Papenhuijzen, Rheol. Acta **11**, 73 (1972).
[7] M. van den Tempel, J. Colloid Interface Sci. **71**, 18 (1979).
[8] H. Kamphuis, R. J. J. Jongschaap, and P. F. Mijnlieff, Rheol. Acta **23**, 329 (1984).
[9] H. Kamphuis and R. J. J. Jongschaap, Colloid Polym. Sci. **263**, 1008 (1985).
[10] R. Vreeker, L. L. Hoekstra, D. C. den Boer, and W. G. M. Agteroff, Colloids Surf. **65**, 185 (1992).
[11] S. S. Narine and A. G. Marangoni, Phys. Rev. E **59**, 1908 (1999).
[12] A. J. Haighton, J. Am. Oil Chem. Soc. **36**, 345 (1959).
[13] F. Shama and P. Sherman, J. Texture Stud. **1**, 196 (1970).

[14] S. S. Davis, J. Texture Stud. **4**, 15 (1973).
[15] D. Rousseau, A. R. Hill, and A. G. Marangoni, J. Am. Oil Chem. Soc. **73**, 983 (1996).
[16] W. W. Christie, *Lipid Analysis—Isolation, Separation, Identification and Structural Analysis of Lipids* (Pergamon, Oxford, 1982).
[17] D. Chapman, Chem. Rev. **62**, 433 (1962).
[18] K. Larsson, Acta Chem. Scand. **20**, 2255 (1966).
[19] J. Yano, F. Kaneko, M. Kobayashi, D. R. Kodali, D. M. Small, and K. Sato, J. Phys. Chem. B **101**, 8112 (1997).
[20] J. Yano, F. Kaneko, M. Kobayashi, and K. Sato, J. Phys. Chem. B **101**, 8120 (1997).
[21] R. E. Timms, Prog. Lipid Res. **23**, 1 (1984).
[22] A. J. Haighton, L. F. Vermas, and C. den Hollander, J. Am. Oil Chem. Soc. **48**, 7 (1971).
[23] B. L. Madison and R. C. Hill, J. Am. Oil Chem. Soc. **55**, 328 (1978).
[24] M. A. J. S. van Boekel, J. Am. Oil Chem. Soc. **58**, 768 (1981).
[25] D. Waddington, in *Fats and Oils: Chemistry and Technology*, edited by R. J. Hamilton and A. Bhati (Applied Science, London, 1980).
[26] D. A. Weitz and M. Oliveria, Phys. Rev. Lett. **52**, 1433 (1983).
[27] W. D. Brown and R. C. Ball, J. Phys. A **18**, L517 (1985).
[28] M. Matshushita, K. Mumida, and Y. Sawada, J. Phys. Soc. Jpn. **54**, 2786 (1985).
[29] W. D. Brown, Ph.D, thesis, University of Cambridge, 1987.
[30] R. C. Sonntag and W. B. Russel, J. Colloid Interface Sci. **116**, 485 (1987).
[31] R. Buscall, P. D. A. Mills, J. W. Goodwin, and D. W. Lawson, J. Chem. Soc., Faraday Trans. **84**, 4249 (1988).
[32] R. C. Ball, Physica D **38**, 13 (1989).
[33] L. G. B. Bremer, T. van Vliet, and P. Walstra, J. Chem. Soc., Faraday Trans. **85**, 3359 (1989).
[34] W. H. Shih, W. Y. Shih, S. I. Kim, J. Lin, and I. A. Aksay, Phys. Rev. A **42**, 4772 (1990).
[35] N. B. Uriev and I. Ya. Ladyzhinsky, Colloids Surf., A **108**, 1 (1996).
[36] B. B. Mandelbrot, *The Fractal Geometry of Nature* (Freeman, New York, 1982).
[37] S. S. Narine and A. G. Marangoni, J. Cryst. Growth **198/199**, 1315 (1999).
[38] S. S. Narine and A. G. Marangoni, J. Am. Oil Chem. Soc. **76**, 7 (1999).
[39] S. F. Edwards and R. B. S. Oakeshott, Physica D **38**, 88 (1989).
[40] I. Heertje, M. Leunis, W. J. M. van Zeyl, and E. Berends, Food Microstruct. **6**, 1 (1987).
[41] A. C. Juriaanse and I. Heertje, Food Microstruct. **7**, 181 (1988).
[42] I. Heertje, Food Struct. **12**, 77 (1993).
[43] R. Jullien and R. Botet, *Aggregation and Fractal Aggregates* (World Scientific, Singapore, 1987).
[44] M. J. J. Vold, J. Colloid Sci. **9**, 451 (1951).
[45] H. C. Hamaker, Physica (Amsterdam) **10**, 1058 (1937).
[46] P. G. de Gennes, *Scaling Concepts in Polymer Physics* (Cornell University Press, Ithaca, NY, 1979).
[47] G. Dietler, C. Aubert, D. S. Cannell, and P. Wiltzius, Phys. Rev. Lett. **57**, 3117 (1986).
[48] J. M. de Man (unpublished).
[49] A. J. Haighton, J. Am. Oil Chem. Soc. **53**, 397 (1976).
[50] P. Sherman (unpublished).
[51] H. Mulder, *Zuivelonderzoek Volume II* (Algemeene Nederlandsche Zuivelbond FNZ, The Hague, 1947).
[52] J. M. de Man, J. Dairy Res. **28**, 117 (1961).
[53] J. M. de Man, Dairy Indus. **29(4)**, 244 (1964).
[54] H. Mulder and P. Walstra, *The Milk fat globule—Emulsion science as applied to milk products and comparable foods* (Centre for Agricultural Publishing, Wagningen, The Netherlands, 1974), pp. 33–53.
[55] J. Foley and J. P. Brady, J. Dairy Res. **51**, 579 (1984).
[56] M. Kawanari, Informatica **10(7)**, 1104 (1996).
[57] G. Cornily and M. leMeste, J. Texture Stud. **16**, 383 (1985).
[58] C. W. Hoerr and D. F. Waugh, J. Am. Oil Chem. Soc. **32**, 37 (1955).
[59] C. W. Hoerr, J. Am. Oil Chem. Soc. **37**, 539 (1960).